Journal of Structural Chemistry. Vol. 58, No. 7, pp. 1324-1331, 2017.
Original Russian Text © 2017 F. Zafarnia, R. Ghiasi, S. Jamehbozorgi.

COMPUTATIONAL STUDY OF OSMABENZYNE: THE SOLVENT EFFECTS ON THE STRUCTURE AND SPECTROSCOPIC PROPERTIES (IR, NMR)

F. Zafarnia[1], R. Ghiasi[2], and S. Jamehbozorgi[3]

UDC 541.6:547.021

In this article, the structural, electronic, and spectroscopic properties of osmabenzyne $Os\{\equiv CC(SiH_3)=C(CH_3)C(SiH_3)=CH\}Cl_2(PH_3)_2$ are explored in the gas phase and five solvents. The effects of solvents on the structural parameters, frontier orbital energies, and spectroscopic parameters of the complex are elucidated using the polarizable continuum model. The wavenumbers of selected IR-active vibrations in different solvents are obtained and correlated with the Kirkwood–Bauer–Magat equation. In addition, thermodynamic parameters of solvation are calculated for the complex. ^1H and ^{13}C NMR chemical shifts are estimated using the gauge-invariant atomic orbital method.

DOI: 10.1134/S0022476617070083

Keywords: metallabenzyne, osmabenzyne, ^1H NMR chemical shift, solvent effect, infrared spectrum.

INTRODUCTION

Benzyne acts as a transient intermediate in an extensive range of chemical transformations. The isolobal transition metal substitution for a carbon atom or a C–H group in benzyne leads to the formation of a metallabenzyne. Hence, one expects that the synthesis of stable metallabenzynes seems impractical. The first stable metallabenzyne $[Os(\equiv CC(SiMe_3)=C(CH_3)C–(SiMe_3)=CH)Cl_2(PPh_3)_2]$ was obtained inexpertly during efforts to prepare osmium vinylidene complexes of the type $[OsCl_2(=C=CHR)(PR'_3)_2]$ [1]. Various stable metallabenzynes have extensively attracted attention and their attractive chemical properties have been explored [2-8]. The chemistry of metallabenzynes has been surveyed in several reviews [9-12]. Metallabenzynes can undergo electrophilic substitution reactions to give new metallabenzynes [13], nucleophilic addition reactions to give metallabenzenes [5] or isometallabenzenes [14], and migratory insertion reactions to give carbene complexes [15-17]. Furthermore, the rearrangement of metallabenzynes to chlorocyclopentadienyl has been reported [18].

The electronic rationalization for the stabilization of osmabenzyne has been studied with the aid of the orbital interaction analysis and density functional theory calculations [8]. Moreover, we have theoretically studied the substituent effect on the structure and properties of osmabenzyne [19].

[1]Department of Chemistry, Faculty of Science, Arak Branch, Islamic Azad University, Arak, Iran. [2]Department of Chemistry, East Tehran Branch, Islamic Azad University, Tehran, Iran; rezaghiasi1353@yahoo.com. [3]Department of Chemistry, Faculty of Science, Hamedan Branch, Islamic Azad University, Hamedan, Iran. The text was submitted by the authors in English. *Zhurnal Strukturnoi Khimii*, Vol. 58, No. 7, pp. 1364-1370, September-October, 2017. Original article submitted December 24, 2015; revised February 11, 2016.

 0022-4766/17/5807-1324 © 2017 by Pleiades Publishing, Ltd.

A solvent plays a significant role in physical and chemical processes. The specific and non-specific interactions between the solvents and the solute molecules alter numerous properties such as the molecular geometry, electronic structure, and dipole moment of the solute.

The major aim of the present investigation is to clarify the solvent effect on the structural, electronic, and IR-active vibrational frequencies and ^{1}H, ^{13}C NMR of osmabenzyne Os{≡CC(SiH_3)=C(CH_3)C(SiH_3)=CH}$Cl_2(PH_3)_2$ (**1**).

COMPUTATIONAL METHODOLOGY

All calculations were performed at the DFT level with the modified Perdew-Wang exchange and correlation (MPW1PW91) method [20]. The standard 6-311G(*d*,*p*) basis set was used for the main group elements (C, H, Si, Cl and P) [21-24]. For osmium, the Def2-TZVPPD basis set [25] and the effective core potential (ECP) of Wadt and Hay [26] were employed. Complex **1** has the singlet ground state taking into account the Os electronic configuration. Frequency calculations were performed to confirm the nature of the stationary points.

To study the effect of solvents, all structures were re-optimized in solutions using the polarizable continuum model (PCM) [27], which includes non-electrostatic effects. In this model, the solvent is modeled by a continuum of uniform permittivity. The solute is placed in a cavity defined as the union of a series of overlapping spheres centered on heavy atoms.

^{13}C and ^{1}H chemical shifts were calculated relative to TMS using the gauge independent atomic orbital (GIAO) method [28] at the same level of theory. The GIAO method is one of the most well-known approaches for the calculation of nuclear magnetic shielding tensors. The Gaussian 09 suite of programs [29] was used in the calculations.

RESULTS AND DISCUSSION

Dipole moments. Fig. 1 represents the structure and numbering scheme for the osmabenzyne complex used in the calculations. Table 1 gathers the calculated dipole moments of the osmabenzyne complex in vacuum and various solvents. The calculated dipole moments show that these values are larger in the solution phase than in the vacuum. On the other hand, the dipole moments enhance along with increasing dielectric constant of solvents. There is a linear correlation between the values of dipole moments and dielectric constant:

$$\mu = 0.1798\varepsilon + 9.1253, \quad R^2 = 0.9757.$$

Polarizability. Polarizability is the measure of the distortion of a molecule in an electric field. Table 1 shows isotropic and anisotropic polarizability values of the studied osmabenzyne complex in vacuum and different solvents. As can be observed, isotropic and anisotropic polarizability values enhance along with increasing dielectric constant of solvents. There is a good relationship between isotropic polarizability values and dielectric constants

$$\alpha_{iso} = 3.4799\varepsilon + 299.81, \quad R^2 = 0.9749,$$

$$\alpha_{aniso} = 0.7894\varepsilon + 109.6, \quad R^2 = 0.9544.$$

Thus, the solvent effect on the isotropic and anisotropic polarizability is in parallel with that on the dipole moment of the solute. Namely, the larger the dipole moment of a solute, the higher the isotropic and anisotropic polarizabilities in the more polar solvents.

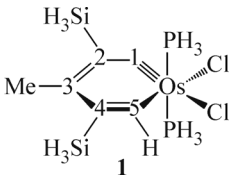

1

Fig. 1. Molecular structure and atomic numbering of studied osmabenzyne.

TABLE 1. Total Dipole Moment (Debye), Isotropic Polarizability (a.u.) of Complex **1** in the Gas and Solution Phases (ε is the dielectric constant of the solvent)

Phase	ε	μ	α_{iso}	α_{aniso}
Gas	–	6.5937	246.32	84.56658
$CHCl_3$	4.71	9.90	314.67	112.84
PhCl	5.70	10.19	320.44	114.37
THF	7.43	10.55	327.42	116.00
DMS	9.60	10.85	333.08	117.13
DCE	10.13	10.90	334.13	117.32

Structural parameters. Table 2 shows the structural parameters of the studied osmabenzyne complex in vacuum and different solvents. It is evident that the C2–C3, Os–P, and Os–Cl bond lengths are longer in the solution phase than in the gas phase. On the other hand, these bonds lengthen along with increasing dielectric constant of solvents. There is a good relationship between the bond lengths and dielectric constants (Table 2).

The Os–C1, C1–C2, C4–C5, and C5–Os bond distances are shorter in the solution phase than in the gas phase. On the other hand, these bonds shorten with increasing dielectric constant of the solvents. There is a good relationship between the values of these bond distances and the dielectric constants (Table 2).

Most optimized bond lengths are slightly larger than the experimental values [8]. Since the theoretical calculations correspond to isolated molecules in the gas phase, the experimental results correspond to molecules either in the solid state or solutions [30].

Molecular orbital analysis. The values of frontier orbital energies, hardness, chemical potential and electrophilicity of the studied osmabenzynes are listed in Table 3. According to the calculations, the inclusion of solvation effects leads to changes in the molecular orbital energies (Table 3). In the solution, HOMO is stabilized with respect to the corresponding

TABLE 2. Selected Bond Lengths in the Optimized Structure of Complex **1** in the Gas and Solution Phases (Å). R^2 Values are the Correlation Coefficients for the Linear Dependence of these Values on the Dielectric Constants of Solvents

Phase	Os–C1	C1–C2	C2–C3	C3–C4	C4–C5	C5–Os	Os–P	Os–Cl1	Os–Cl5
Gas	1.7599	1.3690	1.4090	1.4315	1.3899	2.0259	2.3629	2.4706	2.4524
$CHCl_3$	1.7565	1.3655	1.4102	1.4333	1.3882	2.0213	2.3743	2.4948	2.4789
PhCl	1.7563	1.3651	1.4103	1.4334	1.3879	2.0209	2.3750	2.4970	2.4813
THF	1.7561	1.3647	1.4104	1.4336	1.3877	2.0205	2.3759	2.4995	2.4841
DMS	1.7559	1.3643	1.4105	1.4337	1.3875	2.0203	2.3765	2.5016	2.4864
DCE	1.7559	1.3642	1.4105	1.4337	1.3874	2.0202	2.3766	2.5020	2.4869
R^2	0.9624	0.9752	0.9578	0.9758	0.9798	0.9615	0.9695	0.9736	0.9746

TABLE 3. Frontier Orbital Energies (HOMO and LUMO, Hartree), Hardness (eV), Chemical Potential (eV) and Electrophilicity (eV) of Complex **1** in the Gas and Solution Phases

Phase	*E*(HOMO)	*E*(LUMO)	Δ*E*	η	μ	ω
Gas	–0.2395	–0.0999	3.797	1.899	–4.618	5.615
$CHCl_3$	–0.2418	–0.0983	3.906	1.953	–4.628	5.483
PhCl	–0.2420	–0.0982	3.914	1.957	–4.629	5.474
THF	–0.2422	–0.0980	3.923	1.962	–4.629	5.462
DMS	–0.2424	–0.0979	3.931	1.965	–4.629	5.452
DCE	–0.2424	–0.0979	3.932	1.966	–4.629	5.450

values in vacuum. The HOMO stability enhances together with increasing solvent polarity. A good linear relation is seen between the HOMO energy and dielectric constants

$$E(\text{HOMO}) = -1\cdot10^{-4}\varepsilon - 0.2414, \quad R^2 = 0.9566.$$

In the solution, LUMO is destabilized with respect to the corresponding values in vacuum. The LUMO stability reduces with increasing solvent polarity. A good linear relation is seen between the HOMO energy and dielectric constants

$$E(\text{LUMO}) = 8\cdot10^{-5}\varepsilon - 0.0986, \quad R^2 = 0.983.$$

Hardness values of the complex in solvated media are greater than the corresponding values computed in vacuum. These values enhance in more polar solvents. A good linear relation is seen between the hardness and the dielectric constants

$$\eta = 0.0024\varepsilon + 1.9429, \quad R^2 = 0.97.$$

The study of the solvent effect on the chemical potential values indicates these values are larger in the solution phase than in the gas phase. These values increase with increasing solvent polarity.

On the other hand, the study of the solvent effect on the electrophilicity shows that these values increase in the solution phase as compared to the gas phase. The electrophilicity values increase with increasing dielectric constants. As seen from Table 3, there is a good linear relation between the electrophilicity and the dielectric constant

$$\omega = -0.006\varepsilon + 5.5093, \quad R^2 = 0.9806.$$

Vibrational spectrum analysis. The studied osmabenzyne belongs to the C1 point symmetry group. This complex consists of 29 atoms and is characterized by 81 normal modes of fundamental vibrations. The wavenumbers of the most intense IR bands for the title osmabenzyne complex are given in Table 4 in the gas phase and various solvents. These vibrations are shown in Fig. 2.

1. The C1–C2 and C4–C5 stretching vibrations generally give rise to a band at 1548.20 cm^{-1} in the gas phase. These wavenumbers increase along with increasing solvent polarity.

2. The SiH_3 stretching vibrations appear to be at 2212.06 cm^{-1}, 2229.45 cm^{-1}, 2231.06 cm^{-1}, and 2208.59 cm^{-1} in the gas phase. The first and the second of these vibrations result from the symmetric stretching of SiH_3 modes in which three Si–H bonds of the silyl group are extended. These wavenumbers increase with increasing solvent polarity. The third and the fourth vibrations are due to the asymmetric stretching modes of the silyl group. One of the Si–H bonds of the silyl group is extended, while the other one is contracted.

3. The bending vibrations of the SiH_3 group appeare at 927.30 cm^{-1}, 936.81 cm^{-1}, and 963.18 cm^{-1} in the gas phase. Two bending vibrations can occur within a silyl group. These wavenumbers decrease with increasing solvent polarity. The first of these vibrations (the symmetrical bending vibration) involves the out-of-phase bending of the Si–H bonds. The symmetric and asymmetric bendings of two silyl groups together lead to two bands appearing at 927.30 cm^{-1} and 936.81 cm^{-1} in the gas phase, respectively. The second vibration is an asymmetric bending in the silyl group. The symmetric vibration of this type for two silyl groups together give rise to a band at 963.18 cm^{-1}.

TABLE 4. IR-Active Stretching Wavenumber of the Selected Vibration of the Studied Osmabenzyne Complex in the Gas and Solution Phases (cm^{-1}). R^2 (a) and R^2 (b) Values are the Correlation Coefficients for the Dependence of these Values on ε and $(\varepsilon - 1)/(2\varepsilon+1)$, Respectively

Vibration	υ_{42}	υ_{44}	υ_{48}	υ_{49}	υ_{65}	υ_{66}	υ_{67}	υ_{68}	υ_{69}
Gas	927.30	936.81	963.18	1001.99	1548.20	2208.59	2212.06	2229.45	2231.06
$CHCl_3$	910.71	927.46	957.41	993.11	1549.82	2209.75	2215.09	2235.09	2236.60
PhCl	909.56	926.51	956.92	992.52	1550.10	2209.93	2215.40	2235.67	2237.12
THF	908.23	925.36	956.32	991.78	1550.48	2210.14	2215.77	2236.35	2237.73
DMS	907.18	924.36	955.84	991.13	1550.74	2210.33	2216.09	2236.93	2238.22
DCE	906.99	924.17	955.75	990.99	1550.79	2210.37	2216.15	2237.03	2238.30
R^2 (a)	0.9704	0.98	0.9747	0.9829	0.9694	0.9804	0.9788	0.9769	0.9712
R^2 (b)	1.000	0.998	0.999	0.997	0.999	0.998	0.998	0.999	0.999

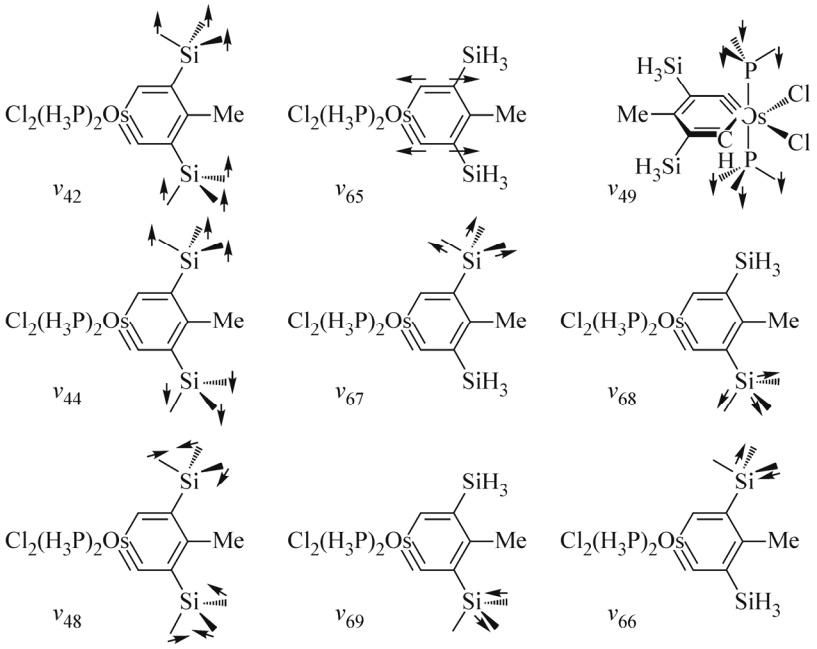

Fig. 2. IR-active selected vibrational modes of studied osmabenzyne.

4. The bending vibrations of PH_3 groups show a band at 11001.99 cm^{-1} in the gas phase. The symmetrical bending vibration involves the out-of-phase bending of P–H bonds. The asymmetric bending of two phosphine groups together gives rise to this band. These wavenumbers decrease with increasing solvent polarity.

Kirkwood–Bauer–Magat (KBM) equation. The first theoretical treatment of the solvent-induced stretching frequency shifts was given by KBM and is described by the following equation:

$$\frac{(\nu_{gas} - \upsilon_{sol})}{\nu_{gas}} = \frac{\Delta\upsilon}{\nu_{gas}} = \frac{C(\varepsilon - 1)}{(2\varepsilon + 1)}.$$

where ν_{gas} is the vibrational frequency of a solute in the gas phase, υ_{sol} is the frequency of a solute in the solvent, ε is the dielectric constant of the solvent and C is a constant depending on the dimensions and electrical properties of the vibrating solute dipole.

Table 4 indicates that the solvent-induced stretching vibrational frequency shifts have good correlation with the KBM equation.

Thermodynamic parameters. Absolute free energy and enthalpy values of the osmabenzyne complex are listed in Table 5. The solvation free energy and enthalpy values are computed via the following equation:

$$\Delta X_{solv} = X_{solv} - X_{gas}, \quad X = G, H.$$

Table 5 reports that the absolute values of ΔG_{solv} and ΔH_{solv} of osmabenzyne decrease with increasing dielectric constant. A typical correlation of the free energy of solvation (ΔG_{solv}) of a molecule with the dipole moment and the dielectric constant is described by the Kirkwood–Onsager model. The Kirkwood expression [31] relates the standard Gibbs free energy of transfer of a spherical dipolar molecule of radius r and dipole moment μ from the gas phase (ε = 1) to a continuous medium (with ε > 1) according to

$$\Delta G_{solv} = -\frac{N_A}{4\pi \cdot \varepsilon_0} \cdot \frac{\mu^2}{r^3} \cdot \frac{\varepsilon - 1}{2\varepsilon + 1}.$$

For the studied osmabenzyne the dependence of ΔG_{solv} versus $\mu^2 \cdot (\varepsilon - 1)/(2\varepsilon + 1)$ of the Kirkwood–Onsager model indicates a linear correlation between these ΔG_{solv} and $\mu^2 \cdot (\varepsilon -)/(2\varepsilon + 1)$:

$$\Delta G_{solv} = -2.510 \cdot (\varepsilon - 1)/(2\varepsilon + 1) - 1.72, \quad R^2 = 0.999.$$

TABLE 5. Calculated Thermodynamic Parameters of the Studied Osmabenzyne Complex in the Gas and Solution Phases (G and H in a.u., ΔG_{solv} in kcal/mol)

Phase	G	H	ΔG_{solv}	Phase	G	H	ΔG_{solv}
Gas	–2511.178	–2511.103	0.00	THF	–2511.198	–2511.122	–12.44
$CHCl_3$	–2511.195	–2511.120	–10.59	DMS	–2511.199	–2511.124	–13.32
PhCl	–2511.196	–2511.121	–11.40	DCE	–2511.199	–2511.124	–13.49

^{1}H and ^{13}C NMR spectra. The ^{1}H and ^{13}C NMR spectral data for the studied osmabenzyne complex are compiled in Table 6. These values reveal signals for carbon atoms at 327.85 ppm (C1), 95.95 ppm (C2), 189.17 ppm (C3), 128.94 ppm (C4), and 257.80 ppm (C5) in the gas phase. In various solvents, the C5 chemical shifts decreased. However, the chemical shifts of C1, C2, C3, and C4 increased. The signal for the H5 atom was observed at 13.83 ppm (H3) in the gas phase. This chemical shift decreased in different solvents.

Table 6 complies the theoretical and experimental [3] ^{1}H and ^{13}C NMR chemical shifts of the title compound. There are linear relationships between the experimental and theoretical values (Table 6).

The dependence of chemical shifts on the solvent dielectric constants is investigated, and there are good relationships between these shifts and the dielectric constant (Table 6). The chemical shifts of C1, C2, C3, and C4 increase with increasing polarity of solvents. Conversely, the chemical shifts of C5 and H5 decrease with increasing polarity of solvents.

The dependence of the chemical shifts of carbon and hydrogen atoms in the studied osmabenzyne complex on $(\varepsilon - 1)/(2\varepsilon + 1)$ of the KBM equation indicates a linear correlation between these chemical shifts and KBM parameters. These equations are as follows:

$$\delta(C1) = 9.041(\varepsilon - 1)/(2\varepsilon + 1) + 325.9, \quad R^2 = 0.996;$$
$$\delta(C2) = 2.803(\varepsilon - 1)/(2\varepsilon + 1) + 95.90, \quad R^2 = 0.936;$$
$$\delta(C3) = 19.59(\varepsilon - 1)/(2\varepsilon + 1) + 187.2, \quad R^2 = 0.999;$$
$$\delta(C4) = 5.120(\varepsilon - 1)/(2\varepsilon + 1) + 128.4, \quad R^2 = 0.982;$$
$$\delta(C5) = -14.97(\varepsilon - 1)/(2\varepsilon + 1) + 260.3, \quad R^2 = 0.993;$$
$$\delta(H5) = -0.705(\varepsilon - 1)/(2\varepsilon + 1) + 12.34, \quad R^2 = 0.922.$$

TABLE 6. ^{1}H and ^{13}C NMR Chemical Shifts of the Studied Osmabenzyne Complex in the Gas and Solution Phases (ppm, TMS). R^2 (a) and R^2 (b) Values are the Correlation Coefficients for the Dependence of Chemical Shifts on the Experimental Values and the Dielectric Constants of Solvents, Respectively

Phase	C1	C2	C3	C4	C5	H5	R^2 (a)
exp*	306.60	136.10	188.60	136.10	227.80	13.83	–
Gas	327.85	95.95	189.17	128.94	257.80	12.19	**0.966**
$CHCl_3$	329.16	96.89	194.26	130.24	255.01	12.09	**0.969**
PhCl	329.36	96.97	194.70	130.37	254.71	12.08	**0.970**
THF	329.64	97.08	195.25	130.54	254.36	12.07	**0.970**
DMS	329.78	97.08	195.61	130.59	253.97	12.04	**0.970**
DCE	329.82	97.10	195.70	130.62	253.92	12.04	**0.970**
R^2 (b)	**0.951**	**0.834**	**0.963**	**0.917**	**0.988**	**0.995**	–

* The values reported for CD_2Cl_2. T. B. Wen, Z. Y. Zhou, and G. Jia, *Angew. Chem. Int. Ed.*, **40**, 1951 (2001).

CONCLUSIONS

A computational investigation has been performed to investigate the solvent effect on the structure and properties of the osmabenzyne complex. The theoretical chemical shifts in the ^{13}C and ^{1}H NMR spectra are compatible with the experimental results. ΔG_{solv} and ΔH_{solv} values increased in more polar solvents. A good linear correlation is observed between the wavenumber of the selected stretching band of the complex and the KBM solvent parameters.

REFERENCES

1. G. P. Elliott, W. R. Roper, and J. M. Waters, *J. Chem. Soc. Chem. Commun.*, 811 (1982).
2. J. Chen, H. H. Y. Sung, I. D. Williams, Z. Lin, and G. Jia, *Angew. Chem. Inter. Ed.*, **50**, 10675 (2011).
3. T. B. Wen, Z. Y. Zhou, and G. Jia, *Angew. Chem. Int. Ed.*, **40**, 1951 (2001).
4. T. B. Wen, W. Y. Hung, H. H. Y. Sung, I. D. Williams, and G. Jia, *J. Am. Chem. Soc.*, **127**, 2856 (2005).
5. W. Y. Hung, J. Zhu, T. B. Wen, K. P. Yu, H. H. Y. Sung, I. D. Williams, Z. Lin, and G. Jia, *J. Am. Chem. Soc.*, **128**, 13742 (2006).
6. G. He, J. Zhu, W. Y. Hung, T. B. Wen, H. H. Y. Sung, I. D. Williams, Z. Lin, and G. Jia, *Angew. Chem. Int. Ed.*, **46**, 9065 (2007).
7. Y. Huang, X. Wang, K. An, J. Fana, and J. Zhu, *Dalton Trans.*, **43**, 7570 (2014).
8. S.-Y. Yang, X-Y. Li, and Y.-Z. Huang, *J. Organomet. Chem.*, **658**, 9 (2002).
9. G. Jia, *Acc. Chem. Res.*, **37**, 479 (2004).
10. G. Jia, *Coord. Chem. Rev.*, **251**, 2167 (2007).
11. J. Chen and G. Jia, *Coord. Chem. Rev.*, **257**, 2491 (2013).
12. X-Y. Cao, Q. Zhao, Z. Lin, and H. Xia, *Acc. Chem. Res.*, **47**, 341 (2014).
13. T. B. Wen, S. M. Ng, W. Y. Hung, Z. Y. Zhou, M. F. Lo, L. Y. Shek, I. D. Williams, Z. Lin, and G. Jia, *J. Am. Chem. Soc.*, **125**, 884 (2003).
14. Q. Zhao, J. Zhu, Z. A. Huang, X. Y. Cao, and H. Xia, *Chem. Eur. J.*, **18**, 11597 (2012).
15. J. Chen, C. Shi, H. H. Y. Sung, I. D. Williams, Z. Lin, and G. Jia, *Angew. Chem., Int. Ed. Engl.*, **50**, 7295 (2011).
16. C. Anusha, S. De, and P. Parameswaran, *Dalton Trans.*, **42**, 14733 (2013).
17. J. Fan, K. An, X. Wang, and J. Zhu, *Organometallics*, **32**, 6271 (2013).
18. J. Chen, K.-H. Lee, T. Wen, F. Gao, H. H. Y. Sung, I. D. Williams, Z. Lin, and G. Jia, *Organometallics*, **34**, 890 (2015).
19. R. Ghiasi, H. Pasdar, and F. Irajizadeh, *J. Chil. Chem. Soc.*, **60** (2015).
20. C. Adamo and V. Barone, *J. Chem. Phys.*, **108**, 664 (1998).
21. R. Krishnan, J. S. Binkley, R. Seeger, and J. A. Pople, *J. Chem. Phys.*, **72**, 650 (1980).
22. A. J. H. Wachters, *J. Chem. Phys.*, **52**, 1033 (1970).
23. A. D. McLean and G. S. Chandler, *J. Chem. Phys.*, **72**, 5639 (1980).
24. P. J. Hay, *J. Chem. Phys.*, **66**, 4377 (1977).
25. D. Rappoport and F. Furche, *J. Chem. Phys.*, **133**, 134105 (2010).
26. D. Andrae, U. Haeussermann, M. Dolg, H. Stoll, and H. Preuss, *Theor. Chim. Acta*, **77**, 123 (1990).
27. J. Tomasi, B. Mennucci, and R. Cammi, *Chem. Rev.*, **105**, 2999 (2005).
28. K. Wolinski, J. F. Hinton, and P. Pulay, *J. Am. Chem. Soc.*, **112**, 8251 (1990).
29. M. J. Frisch, G. W. Trucks, H. B. Schlegel, G. E. Scuseria, M. A. Robb, J. R. Cheeseman, G. Scalman, V. G. Barone, B. Mennucci, G. A. Petersson, H. Nakatsuji, M. Caricato, X. Li, H. P. Hratchian, A. F. Izmaylov, J. Bloino, G. Zheng, J. L. Sonnenberg, M. Hada, M. Ehara, K. Toyota, R. Fukuda, J. Hasegawa, M. Ishida, T. Nakajima, Y. Honda, O. Kitao, H. Nakai, T. Vreven, J. A. Jr. Montgomery, J. E. Peralta, F. Ogliaro, M. Bearpark, J. J. Heyd, E. Brothers, K. N. Kudin, V. N. Staroverov, R. Kobayashi, J. Normand, K. Raghavachari, A. Rendell, J. C. Burant, S. S. Iyengar, J. Tomasi,

M. Cossi, N. Rega, J. M. Millam, M. Klene, J. E. Knox, J. B. Cross, V. Bakken, C. Adamo, J. Jaramillo, R. Gomperts, R. E. Stratmann, O. Yazyev, A. J. Austin, R. Cammi, C. Pomelli, J. W. Ochterski, R. L. Martin, K. Morokuma, V. G. Zakrzewski, G. A. Voth, P. Salvador, J. J. Dannenberg, S. Dapprich, A. D. Daniels, O. Farkas, J. B. Foresman, J. V. Ortiz, J. Cioslowski, and D. J. Fox, *Revision A.02 ed.*, Gaussian, Inc., Wallingford CT (2009).

30. N. Sundaraganesan, S. Kalaichelvan, C. Meganathan, B. D. Joshua, and J. Cornard, *Spectrochim. Acta Part A*, **71**, 898 (2008).
31. J. G. Kirkwood, *J. Chem. Phys.*, **2**, 351 (1934).